



## Influence of Gold Nanoparticles (GNPs) on Radiofrequency Tissue Heating

Geetha Chakaravarthi <sup>\*(1)</sup>, Ashwin Kumar Narasimhan <sup>(2)</sup>, M. S. Ramachandra Rao <sup>(3)</sup>, Kavitha Arunachalam <sup>(4)</sup>

(1) Department of Instrumentation & Control Engineering, NIT Trichy, India

(2) Department of Biomedical Engineering, Rajalakshmi Engineering College, Thandalam, India.

(3) Nano Functional Materials Technology Centre (NFMTC), Department of Physics, IIT Madras, India

(4) Department of Engineering Design, IIT Madras, India

### Abstract

Radio Frequency (RF) heating of Gold nanoparticles (GNPs) for hyperthermia is presented. RF heating experimental study was carried out at 915 MHz for phosphate buffer solution (PBS) with and without 10 nm GNPs in muscle phantom. Influence of GNPs on radiated heating was investigated for 10 and 20 W input power. The phantom heating rate was similar for the control (only PBS) and PBS with GNPs. Experimental results showed that the buffer solution with and without the GNPs heated alike indicating no enhancement in RF heating.

**Keywords:** gold nanoparticles, radio frequency, heating, thermal therapy

### 1. Introduction

Hyperthermia is clinically demonstrated as an effective adjuvant therapy for cancer treatment when administered with chemotherapy (CT) and radiotherapy (RT) [1-3]. Electromagnetic (EM) tissue heating using high power radio frequency (RF) waves at 915 and 434 MHz is widely practiced for thermal therapy of cancer. There is a growing interest to enhance RF tissue heating using metal nanoparticles when excited at a particular range of EM frequencies [4]. Studies showed that surface plasmon resonance of nano sized metallic particles helps produce heat when exposed to RF wave. Among nanomaterials, gold nano particles (GNPs) have been widely investigated as therapeutic and diagnostic agents due to their chemically inert nature and biocompatibility. Though GNPs are proposed for enhancing RF hyperthermia treatment, their role in RF tissue heating is not clearly understood. The hyperthermia response of GNPs depends on the size, shape, concentration of GNP solution, design of the experiment, and the heating mechanism namely, capacitive, inductive or radiative [5]. Most biocompatible materials like metallic nanomaterials (like Graphene and Gold) and iron clusters with sizes less than 50 nm are used widely for cancer treatment. Phantom experiments suggested that the particles with size greater than 10 nm do not interact to produce heat from Gold nanoparticles

(GNPs) [6]. Smaller diameter GNPs (< 10 nm) heat at nearly twice the rate of larger diameter GNPs ( $\geq 50$  nm), which is attributed to the higher resistivity of smaller gold nanostructures [7].

On the contrary, recent literature suggested that GNPs do not produce any heating effect when exposed to RF wave of 13.56 MHz [8,9]. The role of GNPs on RF heating at 915 MHz has not been reported in literature. Hence, 915 MHz frequency and GNPs of particle size 10 nm, 100  $\mu\text{g/ml}$  were chosen for the study to understand the heating mechanism at 10 and 20 W power levels for superficial hyperthermia. Section II presents the GNPs synthesis, characterization and RF heating experimental set up. Section III presents the RF heating experimental results with and without GNPs. Section IV concludes this work.

### 2. Methodology

GNPs were synthesized by citrate reduction method coated with non-ionic surfactant to avoid aggregation of nanoparticles. The concentration of GNPs was determined by using inductively coupled plasma (ICP-OES) spectroscopy technique. Illustration of the experimental setup for RF heating is shown in Figure 1. RF hyperthermia experimental set-up included a microwave signal source, (antenna and water bolus and fiber optic thermometers (Ipitek, USA) to log phantom temperature and provide feedback to control applicator power. Microwave signal from the signal generator was amplified and transmitted to the antenna through an in-line power meter (Bird Technologies, USA). An acrylamide phantom of 100 mm diameter and height of 50 mm with EM tissue property equivalent to muscle tissue was fabricated with three wells (A, B and C) of 2 ml volume each. The wells were located at a depth of 10 mm from the phantom bottom surface and were heated from the bottom using a water coupled patch antenna. Heating experiments were carried out for PBS and 10 nm GNP dispersed in PBS at 915 MHz and 10 W. Phantom heating experiments were repeated for PBS with and without GNPs and the temperature in the wells loaded with the sample were

logged continuously during the experiments using fiber optic temperature sensors (Channels 1, 2 and 3).

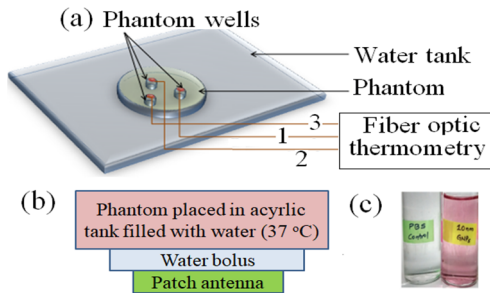


**Figure 1.** Experimental setup for RF heating: (a) 3D setup, (b) side view, and (c) vials containing PBS (sample 1) and 10 nm GNPs dispersed in PBS (sample 2).

### 3. Results and discussion

Figure 2 shows the characterization results of 10 nm GNPs. The synthesized nanoparticles dispersed in phosphate buffer solution (PBS) were characterized as spherical shaped mono-disperse particles with an average size of 10 nm using transmission electron microscopy (TEM). Figures 2a and 2b shows the TEM image at 100 nm zoom and the absorbance spectra of 10 nm tween 20 GNPs. The surface plasmon resonance peak of 10 nm GNPs is located at 524 nm as reported in the literature [10].

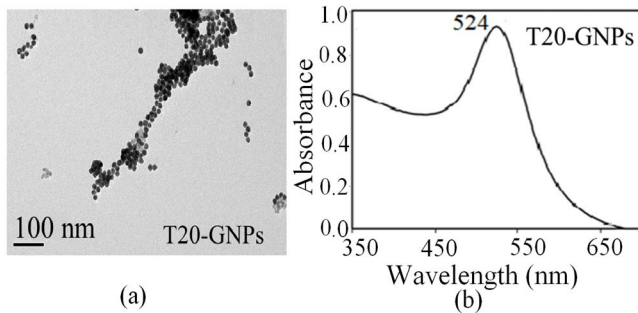


**Figure 2.** Characterization results of synthesised 10 nm GNPs. (a) TEM image and (b) absorbance spectra of T20 GNPs.

Figures 3 show the temperature profiles averaged for three measurements for PBS with and without GNPs exposed at 915 MHz. The temperature rise,  $\Delta T$  logged by thermometry channel 1 for PBS with and without GNPs are 6.17 and 6.26 °C respectively for 20 W power. Table I shows the rise in temperature, at 10 mm muscle depth for both the samples at different power. From table I,  $\Delta T$  for 10 W power are 3.8 and 3.92 °C respectively for PBS with and without GNPs.

Table 1 shows that channel 1 yields higher  $\Delta T$  than channel 2 and 3 for both the samples different power levels. The difference in  $\Delta T$  for different channels is due to the spatial variation in the antenna power deposition pattern. From Table I, it can be observed that the temperature rise is similar for PBS with and without GNPs. Thus, there is negligible effect of GNPs on RF

tissue heating at 915 MHz as reported for low frequency heating in the literature [9]. The slope of the initial steep rise was measured for 1 min to determine the heating rates. Table II shows the averaged heating rate of three channels for both the samples at different power level. In comparison with the PBS, the average heating rate of PBS with GNPs is  $\sim 0.001$  °C/s high, which is insignificant in thermal therapy.

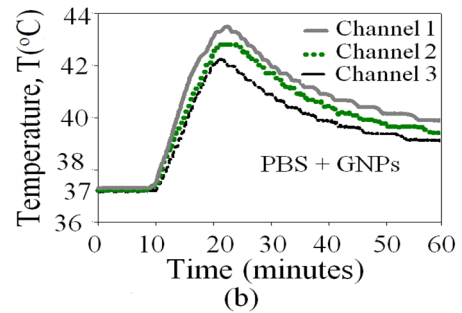
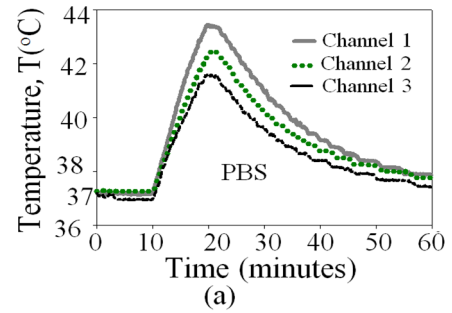


**Figure 3.** RF heating results at 915 MHz. Temperature rise in phantom wells for 20 W RF power for (a) PBS and (b) 10 nm GNPs dispersed in PBS .

**Table I.** Rise in the temperature,  $\Delta T$  for 10 minutes RF heating at 10 mm muscle depth for PBS with and without GNPs.

Fiber optic Sensor	Rise in phantom temperature, $\Delta T$ (°C)			
	PBS		PBS + GNPs	
	10 (W)	20 (W)	10 (W)	20(W)
Channel 1	3.80	6.17	3.92	6.26
Channel 2	3.13	5.52	3.10	5.35
Channel 3	2.55	4.87	2.53	4.93

**Table II.** Averaged heating rate of three channels for both the samples at different power

RF Power (W)	Average heating rate (°C/s)	
	PBS	PBS +GNP
10	0.005	0.006
20	0.009	0.010

## 4. Conclusion

RF heating experiments at 915 MHz indicated no selective increase in heating in the presence of 10 nm size mono-disperse GNPs. Thus, we conclude that the temperature rise observed in this study is primarily due to the conductivity of the PBS and not due to the GNPs. A detailed study of the heating effect of GNPs is under investigation for varying size nano-particles, RF frequency and power level.

## 5. Acknowledgements

The authors thank Sophisticated Analytical Instrument Facility (SAIF), IIT Madras for gold concentration measurements, Department of metallurgical and materials, IIT Madras for TEM images, Department of Biotechnology, IIT Madras for optical property characterization of gold nanomaterials.

## 6. References

1. J. Vander Zee, and D. Gonzalez., "The Dutch deep hyperthermia trial: Results in cervical cancer," *International Journal of Hyperthermia*, 2002,18, pp. 1-12.
2. P. Wust, B. Hildebrandt, G. Sreenivasa, B. Rau, J. Gellermann, H. Riess, R. Felix, and P.M. Schlaq., "Hyperthermia in combined treatment of cancer," *Lancet Oncology*, 2002, 3, pp. 487-97.
3. T. Hehr, P. Wust, M. Bamberg, and W. Budach., "Current and potential role of thermoradiotherapy for solid tumours," *Onkologie*, 2003, 26, pp. 295-302.
4. M.K. Bakht, M. Sadeghi, M. Pourbaghi-Masouleh, C Tenreiro., "Scope of nanotechnology-based radiation therapy and thermotherapy methods in cancer treatment," *Current cancer drug targets*. 2012, 12(8), pp. 998-1015.
5. C.B. Collins, R.S. McCoy, B.J. Ackerson, G.J. Collins and C.J. Ackerson CJ., "Radiofrequency heating pathways for gold nanoparticles". *Nanoscale*, 2014, 6(15), pp. 8459-72.
6. P. Pantano, C.D. Harrison, J. Poulouse, D. Urrabazo , T.Q. Norman and E.I. Braun et al., "Factors affecting the 13.56-MHz radio-frequency-mediated heating of gold nanoparticles," *Applied Spectroscopy Reviews*, 2017, pp. 1-16.
7. S.J. Corr, M. Raof , Y. Mackeyev, S. Phounsavath, M.A. Cheney, and B.T. Cisneros et al., "Citrate-capped gold nanoparticle electrophoretic heat production in response to a time-varying radiofrequency electric-field," *The journal of physical chemistry C, Nanomaterials and interfaces*. 2012,116(45), pp. 24380-9.
8. X. Liu , H.J. Chen, X. Chen , Y. Alfadhil , J. Yu and D. Wen., "Radiofrequency heating of nanomaterials for cancer treatment: Progress, controversies, and future development," *Applied Physics Reviews*. 2015, 2(1), 011103.
9. D. Li , Y. S. Jung , S. Tan, H.K. Kim , E. Chory and D.A. Geller., "Negligible absorption of radiofrequency radiation by colloidal gold nanoparticles," *Journal of colloid and interface science*, 2011, 358(1), pp. 47-53.
10. Y.C. Shih, C.Y. Ke , C.J. Yu, C.Y. Lu and W.L. Tseng., "Combined tween 20-stabilized gold nanoparticles and reduced graphite oxide-Fe<sub>3</sub>O<sub>4</sub> nanoparticle composites for rapid and efficient removal of mercury species from a complex matrix," *ACS applied materials & interfaces* 2014, 6(20), pp.17437-45.